Available online at www.sciencedirect.com
ScienceDirect
Russian Geology and Geophysics 48 (2007) 323–336
RUSSIAN GEOLOGY AND GEOPHYSICS
www.elsevier.com/locate/rgg

New data on kimberlite magmatism in southwestern Angola

K.N. Egorov [a,*], E.F. Roman'ko [b], V.T. Podvysotsky [b], S.M. Sablukov [c], V.K. Garanin [d], D.B. D'yakonov [b]

[a] *Institute of the Earth's Crust, Siberian Branch of the RAS, 128 ul. Lermontova, Irkutsk, 664033, Russia*
[b] *Zarubezhgeologiya Enterprise, 10 Kaloshin per., Moscow, 119002, Russia*
[c] *Central Research Geological Prospecting Institute of Nonferrous and Noble Metals, Russian Academy of Sciences, 129B Varshavskoe shosse, Moscow, 113545, Russia*
[d] *Moscow State University, Vorob'evy Gory, Moscow, 119992, Russia*

Received 10 March 2005; accepted 22 August 2006

Abstract

First data on the geologic and geochemical compositions of kimberlites from nine kimberlite pipes of southwestern Angola are presented. In the north of the study area, there are the Chikolongo and Chicuatite kimberlite pipes; in the south, a bunch of four Galange pipes (I–IV); and in the central part, the Ochinjau, Palue, and Viniaty pipes. By geochemical parameters, these rocks are referred to as classical kimberlites: They bear mantle inclusions of ultrabasites, eclogites, various barophilic minerals (including ones of diamond facies), and diamonds. The kimberlite pipes are composed of petrographically diverse rocks: tuffstones, tuff breccias, kimberlite breccias, autolithic kimberlite breccias, and massive porphyritic kimberlites. In mineralogical, petrographic, and geochemical compositions the studied kimberlites are most similar to group I kimberlites of South Africa and Fe-Ti-kimberlites of the Arkhangel'sk diamondiferous province. Comparison of the mineralogical compositions of kimberlites from southwestern Angola showed that the portion of mantle (including diamondiferous) material of depth facies in kimberlite pipes regularly increases in the S-N direction. The northern diamond-bearing kimberlite pipes are localized in large destructive zones of NE strike, and the central and southern diamond-free pipes, in faults of N-S strike.

Keywords: Kimberlites; diamonds; barophilic minerals; geochemical composition; rare-earth elements; Angola

Introduction

Africa is rich in natural diamond reserves. More than a fifth of them are localized in northeastern Angola, first of all in the Lunda Norte subprovince. Data on kimberlite magmatism and its diamond potential in southwestern Angola are too scarce (Zuev et al., 1988; Roman'ko et al., 2005). There is no information about kimberlite bodies except for their occurrence, which is shown on small-scaled geological maps compiled by Portuguese and South African geologists on diamond prospecting in the 1970s.

In this work we present results of the first complex study of kimberlites from southwestern Angola. The research was carried out by a geological team from the All-Russian Zarubezhgeologiya Enterprise in 2001–04 as part of a contract with Spade Business Ltd, Rulth S.A.R.L., and Instituto Geologico de Angola. Nine kimberlite pipes were stripped and studied (Fig. 1): Chikolongo and Chicuatite in the north, a bunch of four Galange pipes (I–IV) in the south, and Ochinjau, Palue, and Viniaty in the central part.

Regional geology

The above nine kimberlite bodies are localized in the South Angola Shield, on the periphery of the superposed Cenozoic Cunene depression structurally controlled by a system of buried N-S striking faults in rocks of the shield basement. These faults appeared during the formation of the Early Proterozoic Cunene intrusive massif. Within them, the southern (Galange I–IV) and central (Ochinjau, Palue, and Viniaty) groups of kimberlite pipes are localized. The northern group of kimberlite pipes (Chicuatite and Chikolongo) occurs in extended zones of NE-striking faults (Fig. 1).

The Viniaty and Palue kimberlite pipes intrude into Early Proterozoic granites and syenites of the Cibala complex and Chikolongo diatreme; the Chicuatite and Ochinjau pipes, into

* Corresponding author.
E-mail address: egorov@crust.irk.ru (K.N. Egorov)

1068-7971/$ - see front matter © 2007, IGM, Siberian Branch of the RAS. Published by Elsevier B.V. All rights reserved.
doi:10.1016/j.rgg.2006.08.001

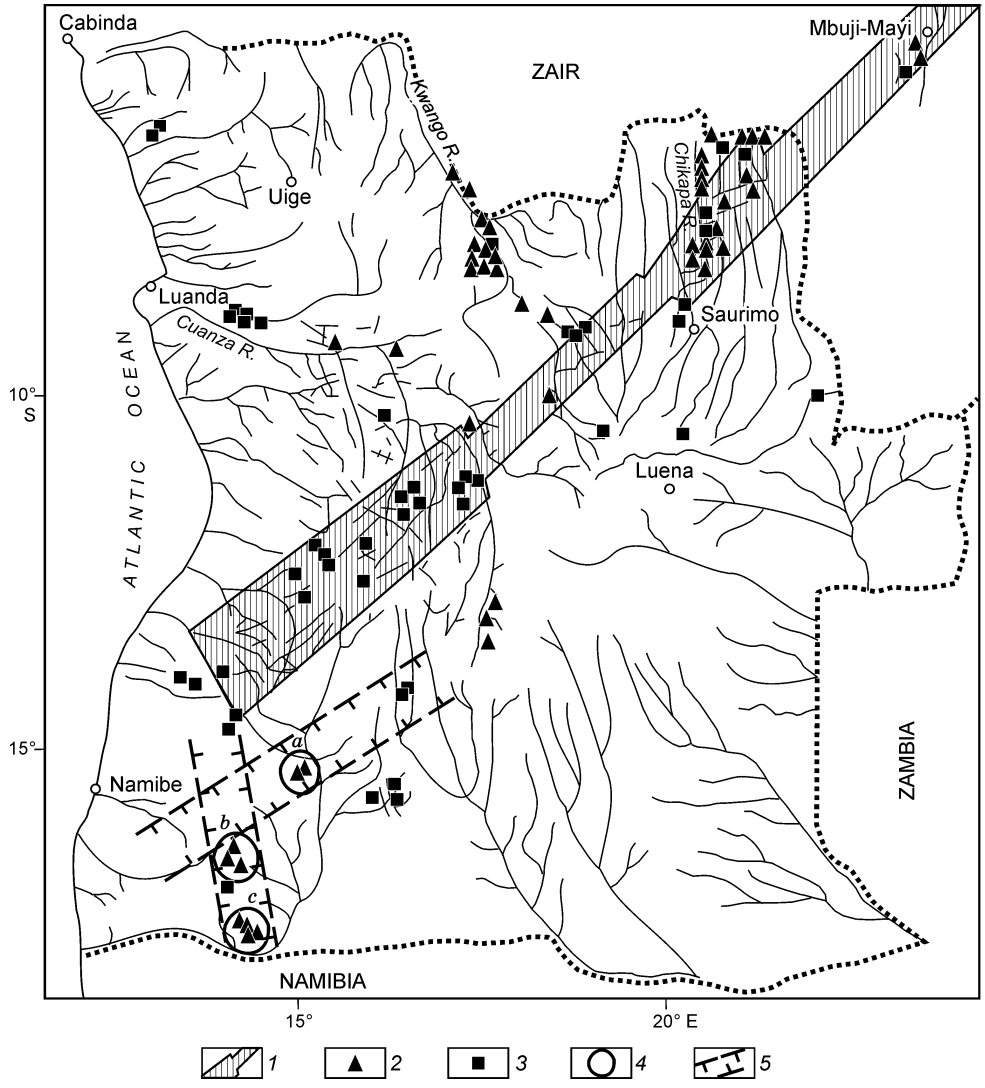

Fig. 1. Schematic occurrence of kimberlite pipes in Angola, after (Zuev et al., 1988), with our supplements. *1* — zone with the maximum concentration of kimberlite bodies and carbonatites; *2* — kimberlites; *3* — carbonatites; *4* — bunches of kimberlite pipes in southwestern Angola: *a* — northern, *b* — central, *c* — southern; *5* — zones of largest faults.

Early Proterozoic anorthosites of the Cunene complex; and the Galange I–IV pipes break through Archean rocks of the South Angola Shield basement.

According to geological and geophysical data, the Chicuatite pipe is drop-shaped, 480×80 m in size; in the northern part it is swollen to 240 m. The Chikolongo pipe is a N-S-striking 240×90 m oval. The Ochinjau and Palue pipes are ellipses 220×80 and 570×140 m in size, respectively. The Galange I pipe is rounded, 64×64 m. The Galange II and III pipes, 130×70 m and 150×100 m in size, respectively, are localized close to each other and are connected by a narrow (20 m) enclosing-rock isthmus at the denudation level. The Galange IV pipe is of intricate shape and N-S strike and is 140×40 m in size.

The presence of crater deposit relics in kimberlite pipes of southwestern Angola evidences a slight diatreme erosion. Volcanosedimentary relics are most abundant in the Chikolongo and Palue pipes.

K-Ar dating of phlogopite from the Chicuatite kimberlite groundmass, which was performed in the Laboratory of Isotope Geology and Geochronology at the Institute of Ore Deposit Geology, Petrography, Mineralogy, and Geochemistry, Moscow, yielded an age of 372±8 Ma. The age was calculated using the following constants: $\lambda_k = 0.581 \cdot 10^{-10}$ year^{-1}, $\lambda_\beta = 4.962 \cdot 10^{-10}$ year^{-1}, and ^{40}K = 0.01167 at.%. The age of the other kimberlite pipes was not determined by radiological methods.

Petrography of kimberlites

By geologic structure, the studied kimberlite pipes are one- (Chicuatite, Galange I–IV), two-, and three-phase (Viniaty, Chikolongo, Ochinjau). They are composed of several rock varieties: tuffstones, tuff breccias, kimberlite breccias, autolithic kimberlite breccias, and massive kimberlite.

Northern group of pipes

The Chikolongo pipe is composed mainly of medium-porphyritic kimberlite with <5% xenogenous material. The xenoliths are fragments of anorthosites, sandstones, limestones, and, seldom, garnet peridotites and pyroxenites.

Porphyritic segregations measuring 2–3 to 8–10 mm are pseudomorphs after olivine (25–30%) as well as diopside (up to 5%), picroilmenite, and pyrope (each, up to 2%). The pseudomorphs after olivine of generations I and II consist of a saponite-serpentine-carbonate aggregate with iron oxide impurity. The fine-scaly groundmass is composed of chlorite, saponite, talc, hydromicas, and occasional grains of perovskite, carbonate, and oxide-ore phases.

In the western part of the Chikolongo pipe, there are relics of crater deposits — obliquely laminated tuffstones. Their terrigenous material includes quartz (25–35%), feldspars (mainly, microcline (5–10%)), and clastics of sedimentary rocks (mainly, siltstones on Fe-containing cement (2–5%)). Kimberlite material occurs in the rock as carbonate pseudomorphs after olivine (10–15%), altered phlogopite (1–2%), ore minerals (1–2%), garnet grains, and occasional fragments of clinopyroxene-bearing mantle inclusions and kimberlites (2–5%). The rock cement (35–40%) is of iron-carbonate-clay composition and contact-pore (locally, basal-pore) texture. The terrigenous clastics are poorly sorted and poorly rounded.

Beneath the tuffstones, red coarse-clastic tuff breccia was discovered. Angular clastics of sandstones, limestones, quartzites, and, more seldom, anorthosites measuring 0.5–1 cm to 7 m amount to >30%. The tuff breccia contains isometric fine-porphyritic autoliths 8–10 mm in size (up to 5%). Pseudomorphs after olivine phenocrysts (10–15%) are thin-sliced saponite. The breccia cement is of iron-sand-clay composition.

The Chicuatite pipe consists mainly of medium-clastic kimberlite breccia; locally, small blocks of fine-porphyritic kimberlite occur. Xenoliths in the breccia amount to no more than 30–40 vol.% of the rock. These are clastics of anorthosites substituted by analcime, natrolite, and pectolite. Mantle inclusions are strongly altered garnet peridotites and ilmenite pyroxenites. The breccia also contains occasional clastics of fine-porphyritic kimberlite, up to 2.5 cm in size. Phenocrysts (40–50%) are pseudomorphs of generation I — large oval grains measuring 1–7 mm. Fine (0.01–0.8 mm) grains of substituted olivine of generation II form intergrowths with perovskite grains. Olivine of generations I and II is substituted by an aggregate of minerals: zeolites (natrolite, pectolite), chlorite, talc, limonite, carbonate, and, seldom, serpentine. Phlogopite phenocrysts are scarce; they are hydrated.

The kimberlite breccia cement is mainly an aggregate of serpentine with fine-scaly mica minerals, oxide-ore phases, and fine-grained carbonate, the latter occurring as accumulations and fine veinlets.

Central group of pipes

The Ochinjau pipe is mainly a bluish-gray fine-clastic breccia with fragments of anorthosites and sandstones (up to 10–15%). Phenocrysts of pseudomorphs after olivine of generation I, consisting of carbonate, serpentine, mica minerals, and iron oxides, amount to 15–20%. The breccia groundmass is a scaly aggregate of mica minerals and carbonate with microcrystals of perovskite, oxide-ore phases, and phlogopite.

On the pipe periphery, the breccia is enriched in unsorted fine-grained terrigenous material: quartz (5–10%) and feldspars (5–7%). The grains are 0.01–0.6 mm in size, angular, and tabular. No rounded grains were found. With depth, the kimberlite breccia passes into an autolithic one containing up to 30% isometric autolith segregations 0.5–3 cm in size.

The Viniaty pipe consists of kimberlite breccia and fine-porphyritic kimberlite with signs of late hydrothermal processes — silicification (presence of chalcedony films and veinlets) and hematite magnetitization. In places, the breccia is strongly silicified and chloritized, so that the rock texture is completely shaded: The kimberlite nature of the breccia is evidenced from the presence of porphyritic segregations of pyrope and picroilmenite. Xenoliths in the kimberlite breccia amount to 15–20%; the rock clastics are granitoids, sandstones, acid effusions, and, more seldom, garnet peridotites. The content of small fragments of fine-porphyritic kimberlite does not exceed 5%. Pseudomorphs after olivine of generation I in the breccia and kimberlite are composed of chlorite, quartz, and iron oxides. The content of pseudomorphs after olivine of generation I is 10–15% in the breccia and 25–30% in the massive kimberlite. The groundmass of the studied rocks is formed by polymineral aggregate of chlorite, quartz, and ore dust. The total content of secondary quartz in the breccia and kimberlite reaches 45–50%.

The surface of **the Palue pipe** is composed of block breccias of the host syenites, whose angular fragments are cemented by clayey sandstone with kimberlite material. In places, there are subhorizontal interbeds and lenses of epiclastic deposits: inequigranular sandstone with small fragments of kimberlite, pyrope and picroilmenite grains, and altered phlogopite plates. The rocks of crater facies overlap a kimberlite tuff breccia stripped at a depth of >4 m. The greenish-pink tuff breccia contains 40 to 80% clastics of red-pink syenites. Inclusions of altered garnet peridotites are occasional. The clayey cement of the tuff breccia contains chlorite and vermiculite laths and scarce grains of pyrope (in kelyphite rims) and Cr-diopside.

Southern group of pipes

The surface of **the Galange I pipe** is composed of altered and weathered tuff breccia. Its xenogenous material includes granite gneisses, schists, and acid effusions. Xenoliths measuring few centimeters to 0.5–0.6 m are angular to oval. There are also scarce mantle inclusions of phlogopite pyroxenites and occasional fragments of fine-porphyritic micaceous kim-

berlite, up to 10 cm in size. Pseudomorphs after olivine of generation I (<10%) consist of microscaly saponite aggregate. Fine (0.01–0.8 mm) grains of olivine of generation II completely replaced by saponite amount to ~25% and are often intergrown with leucoxenized perovskite. The fine-scaly clayey groundmass contains scarce ore-mineral grains and phlogopite laths.

The Galange II pipe is made up of greenish-gray fine- to medium-porphyritic kimberlite with scarce granite-gneiss fragments. The kimberlite is rich in mantle inclusions composed of garnet pyroxenites and peridotites. Pseudomorphs after olivine of generation I (10–15%) are replaced by serpentine, saponite, and carbonate. Phlogopite phenocrysts (1–2%) form oval grains 0.3–1.5 mm in size. Pseudomorphs after olivine of generation II (20–25%) consist of thin-sliced saponite-carbonate aggregate. Note that some kimberlite samples are rich in carbonate pseudomorphs after olivine (up to 70–80%), though the pipe occurs among granite gneisses. Moreover, the kimberlite bears an intense superposed carbonate mineralization expressed as branching thin veinlets. The rock groundmass is composed of hydromica aggregate and contains small grains of perovskite and carbonate, laths of altered phlogopite, and finely disseminated leucoxene.

The Galange III pipe is made up of weathered kimberlite breccia with fragments of granite-gneisses, schists, and, more seldom, sandstones. The mantle inclusions are scarce pyrope serpentinites, and the porphyritic segregations (<10%) are generation I olivine grains completely replaced by saponite. Phlogopite phenocrysts amount to 5–10%. The rock groundmass is formed by a scaly aggregate of saponite with fine grains of leucoxenized perovskite and, more seldom, oxidized ore mineral.

The Galange IV pipe is a strongly weathered, almost completely argillized and carbonatized kimberlite breccia with fragments of granite-gneisses, biotite schists, sandstones, and acid effusions. Mantle inclusions and clastics of early kimberlites were not found.

Olivine of generation I (5–10%) completely replaced by saponite forms large (1–4 to 10 mm) rounded irregular-shaped (with traces of resorption) phenocrysts. The phlogopite phenocrysts (3–5%) are oval pellets 0.3–1.5 mm in size. Locally, phlogopite is intergrown with clinopyroxene and altered olivine. Saponite pseudomorphs after olivine of generation II (30–35%) are small (0.1–1 mm) and euhedral. The rock groundmass is composed of hydromica with scarce grains of perovskite, carbonate, and apatite and laths of altered phlogopite.

Petrochemistry of kimberlites

Most of the studied kimberlites are transformed by hydrothermal-metasomatic and hypergene processes. The intense silicification of the Viniaty kimberlites radically changed not only the initial chemical composition of the rock but also the concentrations of slow-moving (under hypergenesis conditions) elements (Table 1). Therefore, to study the petrochemical composition, we chose kimberlite samples with the minimum degree of secondary alteration and the minimum contamination by xenogenous material. The Chicuatite kimberlites abound in small (<1–2 mm) clastics of anorthosites replaced by zeolites. Therefore, even the samples thoroughly cleaned from xenoliths preserve traces of crustal-material contamination (Table 1). The kimberlites have high contents of Al_2O_3 (9.85–10.9 wt.%) and Na_2O (1.15–1.97 wt.%), with $Na_2O > K_2O$.

A specific petrochemical feature of the studied kimberlites is a low content of MgO and high ones of SiO_2 and Al_2O_3. On the C.I.(crustal-material contamination index)–Ilm.I(Fe-Ti oxide accumulation index) diagram, all composition points of these kimberlites lie beyond the fields of South African micaceous and basaltoid kimberlites (Fig. 2). The high C.I. values (1.4–3.1) of the studied rocks are due mainly to the active removal of MgO during the rock replacement by saponite, talc, chlorite, and zeolites. The highest MgO contents were found in the Chikolongo and Chicuatite kimberlite samples containing serpentine (Table 1).

On the CaO–MgO diagram (Fig. 3, *a*), the studied kimberlites do not form a distinct trend typical of Yakutian kimberlites, first of all because of their contamination with crustal material and the active removal of MgO. Low contents of MgO were found not only in the Ochinjau and Galange II carbonatized kimberlites but also in the samples extremely depleted in carbonate minerals (Table 1).

The high Ilm.I values (0.38–1.05) of the studied kimberlites are due to the high contents of perovskite, ilmenite, and other Fe-Ti oxide minerals in their groundmass. The Ochinjau kimberlites, sample 2938/25 from the Galange I pipe, and sample 401/35 from the Chicuatite pipe are close in Ilm.I. values to aillikites (Fig. 2). By TiO_2–K_2O correlation, the studied kimberlites fall into the field of South African group I kimberlites, except for the Galange I samples corresponding in this parameter to group II kimberlites (Fig. 3, *b*). The studied kimberlites are medium- (1.41–2.7 wt.% TiO_2) and high-titanium (>4.0 wt.% TiO_2) (Bogatikov et al., 2004).

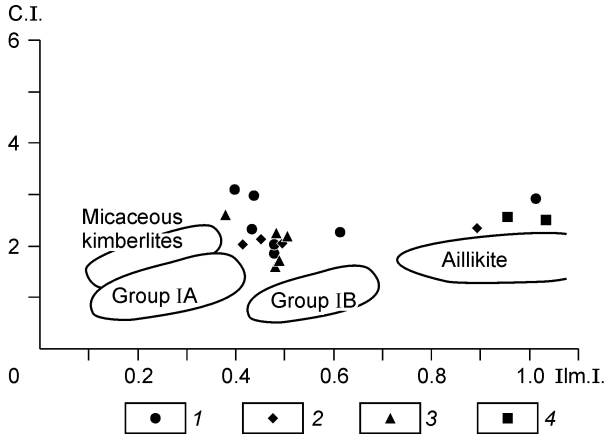

Fig. 2. C.I.–Ilm.I diagram for kimberlites from southwestern Angola, after Taylor et al. (1994). Pipes: *1* — Galange, *2* — Chicuatite, *3* — Chikolongo, *4* — Ochinjau. Fields of Groups IA and IB correspond to basaltoid types of South African kimberlites.

Table 1
Chemical composition (wt.%) of kimberlites from southwestern Angola

Component	Chicuatite pipe		Chikolongo pipe							Ochinjau pipe		Viniaty pipe		Galange I pipe			Galange II pipe		Galange III pipe	Galange IV pipe
	401/42	401/35	401/280	401/302	452/55	452/47.5	452/104	454/60	454/130	Sh-301	Sh-320	7329/26	7329/31	2310	2938/22	2938/25	2937/11	6224	2315	2935/12
SiO_2	35.78	30.68	35.42	34.67	35.78	35.48	42.08	41.46	46.49	37.44	31.98	81.45	90.28	50.37	53.16	43.38	30.56	30.94	43.57	31.87
TiO_2	2.38	4.62	1.52	1.53	2.70	2.40	1.82	2.54	1.41	5.24	4.01	0.74	0.24	1.62	1.42	5.34	2.42	1.97	1.75	1.64
Al_2O_3	10.22	10.50	10.90	9.85	5.08	5.73	5.75	5.03	4.45	6.57	5.70	2.52	1.20	7.67	6.95	5.12	4.10	3.89	5.55	3.30
Fe_2O_3	3.90	6.07	3.24	3.31	5.40	6.95	6.30	6.30	4.73	11.20	8.62	5.81	3.02	6.35	5.02	10.24	5.95	6.39	7.32	5.38
FeO	5.12	5.66	4.88	5.01	4.28	2.55	2.32	1.90	1.42	1.80	1.62	1.50	1.55	0.75	1.42	1.22	1.06	0.65	0.32	1.34
MnO	0.10	0.12	0.10	0.10	0.12	0.10	0.10	0.06	0.10	0.21	0.18	0.02	0.03	0.08	0.10	0.15	0.13	0.12	0.12	0.09
MgO	21.83	17.13	22.12	20.79	24.94	23.80	18.87	18.48	17.23	14.60	12.30	1.37	0.62	13.80	14.96	15.23	14.31	16.95	20.48	16.53
CaO	6.36	9.14	7.08	8.78	8.20	6.56	5.98	5.48	7.15	9.13	17.36	0.56	0.17	3.19	3.30	3.49	18.48	14.33	3.04	16.24
Na_2O	1.35	1.97	1.15	1.83	0.22	0.38	0.84	0.20	0.81	0.41	0.50	0.03	0.04	1.19	0.94	0.08	0.17	0.21	1.19	0.26
K_2O	0.62	0.59	0.58	0.52	0.43	0.27	1.40	1.38	1.34	1.53	1.31	0.27	0.29	3.06	2.38	0.68	0.54	0.92	0.60	0.47
P_2O_5	0.24	0.25	0.20	0.27	0.45	0.44	0.30	0.26	0.30	0.90	0.82	0.14	0.11	0.47	0.46	1.30	0.58	0.51	0.36	0.35
H_2O^-	2.08	1.84	2.75	2.66	2.28	4.50	6.00	9.06	6.03	5.75	3.83	2.63	0.78	7.18	4.93	6.97	4.53	6.30	9.62	2.85
H_2O^+	8.85	7.12	8.94	7.98	7.90	7.80	6.18	4.52	4.90	4.92	5.17	2.83	1.52	3.45	4.80	6.42	5.17	3.94	4.97	6.74
CO_2	0.77	3.42	0.88	1.63	2.53	1.84	1.65	2.56	3.47	0.11	6.16	N.d.	0.11	0.17	N.d.	N.d.	11.66	12.27	0.12	12.76
S_{tot}	N.d.	<0.10	N.d.	0.54	N.d.	<0.10	N.d.	<0.10	N.d.	N.d.	N.d.	N.d.	N.d.	<0.05	N.d.	N.d.	N.d.	<0.05	<0.05	N.d.
Total	99.60	99.68	99.76	99.66	100.31	99.56	99.59	99.59	99.83	99.81	99.56	99.87	99.96	99.33	99.84	99.62	99.66	99.47	99.28	99.82

Note. Analyses were carried out in the Chemical Laboratory of the Institute of the Earth's Crust, Irkutsk (analyst M.N. Smagunova). N.d. — Not determined.

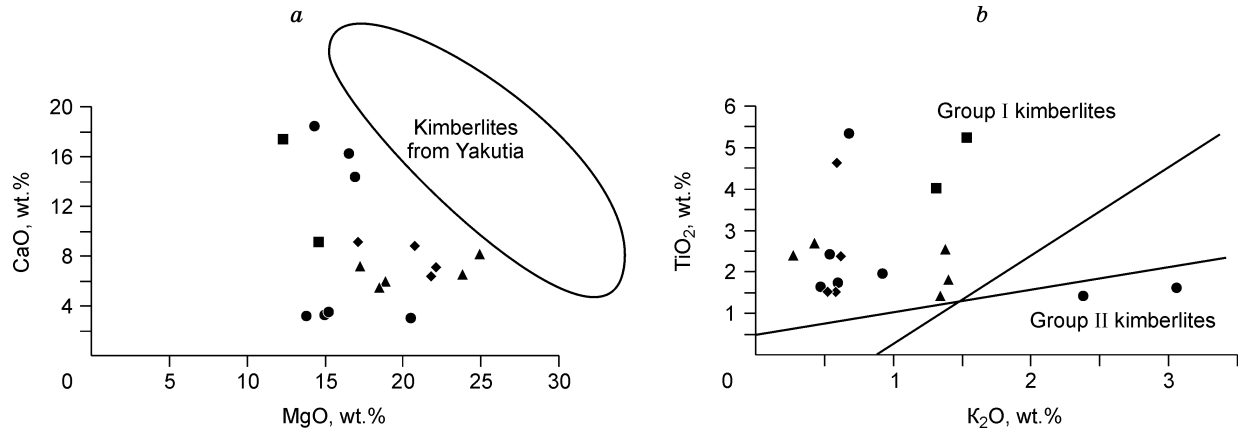

Fig. 3. MgO–CaO (*a*) and K_2O–TiO_2 (*b*) diagrams for kimberlites from southwestern Angola. Designations follow Fig. 2. Fields in (*b*) are given after (Bogatikov et al., 2004).

The concentrations of trace elements in the kimberlites also depend on the intensity of metasomatic and hypergene transformations of the rocks. The silicified Viniaty kimberlites are strongly depleted in all trace elements but Pb, U, and Th (Table 2). The other kimberlites have medium but variable contents of trace elements. The highest contents of Zr (161.58–248.08 ppm), Y (12.84–32.57 ppm), and ΣREE (233.54–430.61 ppm) were found in kimberlites from the Galange I–III and Ochinjau pipes and in sample 452/47.5 from the Chikolongo pipe. These samples have high contents of P_2O_5 (0.36–0.82 wt.%). No other regular relationships between the contents of trace elements and chemical compositions of kimberlites were observed. There is only a direct correlation between the contents of Ta (5.7–14.47 ppm) and TiO_2 (1.53–4.62 wt.%) (Tables 1 and 2).

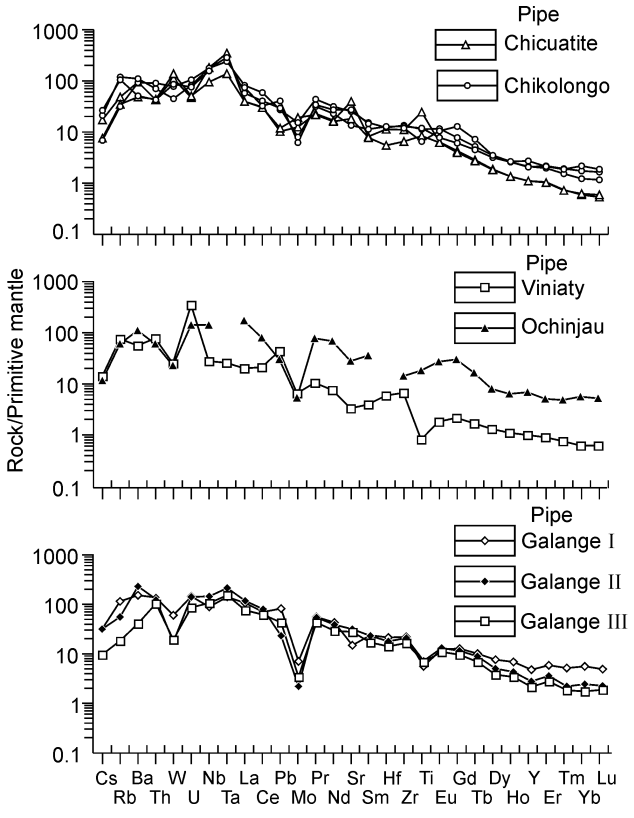

Fig. 4. Primitive-mantle-normalized trace-element patterns (McDonough and Sun, 1995) of kimberlites from southwestern Angola.

By indicator Zr/Nb index (2.27–3.9), the Galange I–III and Viniaty kimberlites belong to South African group II kimberlites (Taylor et al., 1994). The Galange I kimberlites have high values of indicator ratios Ba/Nb (16.91), Rb/Nb (1.14), Ba/La (14.86), and Ba/Th (92.65) and low values of La/Yb (26.28) and Ce/Y (5.67). In these geochemical parameters they are most similar to kimberlites of the Nakyn and Zolotitskoe types (Bogatikov et al., 2001, 2004). Note that on the one hand, the Galange I kimberlites bear chromite–Cr-diopside–pyrope assemblage of indicator minerals and picroilmenite is extremely scarce, and on the other, these rocks are richer in ΣREE (305.55 ppm) as compared with anomalous kimberlites (Bogatikov et al., 2004).

The Chikolongo and Chicuatite kimberlites have medium to high contents of rare alkalies (ppm) — Rb (20–75) and Cs (0.22–0.68) — and alkali-earth elements — Sr (286–841) and Ba (340–771). The contents of HFSE vary from medium to low (ppm): Zr — 72–151, Hf — 1.6–3.9, and Nb — 67–129; the contents of radioactive elements are as follows (ppm): Th — 8.7–11.6 and U — 1.8–3.0. The contents of LREE and HREE vary within 117.65–235.01 ppm. The Chikolongo kimberlites are much richer in REE than the Chicuatite ones.

The spidergrams (Fig. 4) of the Chicuatite kimberlites show distinct W, Nb, Ta, Mo, Sr, and Ti maxima and Pb, Hf, and Zr minima. The distribution curves of all elements from Ta to Mo in all samples have a sharp slope because of the low contents of La and Ce. At the same time, the spidergrams lack a Gd peak typical of kimberlites. These distribution patterns of trace elements (atypical W, Mo, and Eu maxima) are due to the effect of crustal material, which was also revealed in many kimberlites of southwestern Angola, except for sample 454/130 from the Chikolongo pipe and the Ochinjau kimberlites.

The Viniaty silicified kimberlite is strongly depleted in almost all trace elements, but their distribution curve is

Table 2
Contents of trace elements (ppm) in kimberlites from southwestern Angola

Element	Galange I pipe	Galange II pipe	Galange III	Chicuatite pipe		Chikolongo pipe			Viniaty pipe	Ochinjau pipe
	2310	6224	2315	401/35	401/302	452/47.5	454/60	454/130	7329/37	Sh-320
Cs	1.01	1.01	0.31	0.56	0.24	0.22	0.68	0.84	0.46	0.38
Rb	72.83	35.24	11.66	31.05	22.08	20.09	75.87	67.57	48.03	38.63
Ba	1075.41	1598.92	287.52	663.30	340.68	641.12	771.64	359.37	391.71	780.80
Th	11.61	10.74	8.75	3.59	3.70	7.67	5.97	3.64	6.68	5.23
W	1.19	0.35	0.39	2.21	2.77	1.54	0.91	1.73	0.51	0.46
U	3.03	2.93	1.83	0.98	1.07	2.20	1.74	1.61	7.19	2.96
Nb	63.61	102.47	75.23	129.91	67.71	126.09	128.25	111.86	20.42	100.74
Ta	5.83	8.74	6.24	14.47	5.70	9.76	11.75	N.d.	1.07	N.d.
La	72.38	80.62	51.51	27.14	27.49	56.21	39.55	50.84	14.17	117.84
Ce	125.18	141.88	108.78	54.18	52.75	105.14	72.21	56.96	38.44	143.14
Pb	15.02	4.29	7.86	1.91	2.19	4.98	5.46	7.45	8.08	5.59
Mo	0.44	0.14	0.22	0.79	1.20	0.96	0.50	0.39	0.42	0.35
Pr	15.36	14.86	11.90	6.32	5.98	11.97	8.62	9.32	2.97	21.75
Nd	58.27	52.81	39.65	23.13	21.86	43.06	31.04	37.04	10.63	93.90
Sr	312.95	663.21	584.62	841.80	385.26	537.89	286.67	572.94	72.92	602.29
Sm	10.57	10.26	7.61	3.67	3.43	6.74	4.99	6.47	1.81	15.97
Hf	6.58	5.54	4.38	3.52	1.69	3.78	3.96	N.d.	1.90	N.d.
Zr	248.08	233.08	184.49	124.63	72.62	151.63	143.34	132.35	77.51	161.58
Ti	7362.86	9334.54	8865.20	31792.00	10976.00	14746.00	15519.00	8452.95	1115.00	24039.95
Eu	2.08	2.22	1.82	1.08	1.05	1.95	1.30	1.75	0.32	4.66
Gd	7.53	6.86	5.70	2.58	2.34	4.62	3.65	7.74	1.34	18.31
Tb	1.10	0.96	0.73	0.31	0.29	0.57	0.48	0.78	0.19	1.81
Dy	5.66	3.68	2.80	1.37	1.34	2.59	2.33	2.56	1.02	6.03
Ho	1.12	0.71	0.56	0.22	0.22	0.42	0.42	0.44	0.19	1.08
Y	22.08	12.84	9.91	5.06	5.04	9.60	9.43	12.26	4.73	32.57
Er	2.81	1.72	1.33	0.51	0.50	0.94	1.05	1.01	0.46	2.52
Tm	0.38	0.16	0.14	0.06	0.05	0.11	0.14	0.14	0.06	0.37
Yb	2.75	1.19	0.87	0.30	0.31	0.60	0.85	1.06	0.32	2.83
Lu	0.36	0.17	0.14	0.04	0.04	0.09	0.12	0.14	0.05	0.40

Note. Contents of trace elements were determined by ICP MS on a PLASMA QD microprobe at the Institute of Geological Prospecting, Moscow (analyst D.Z. Zhuravlev).

identical to that of the Ochinjau kimberlites (except for the Nb–Pb segment).

The spidergrams of the Galange I–III kimberlites are similar to each other and are gently sloped. These rocks have high contents of Th, U, Ce, and La and low ones of Nb and Ta; therefore, their element patterns are weakly fractionated.

In general, kimberlites of southwestern Angola are most similar in HFSE and REE contents and indicator ratios of trace elements to South African group I kimberlites (Taylor et al., 1994) and Fe-Ti kimberlites of the Arkhangel'sk diamondiferous province (Bogatikov et al., 2000).

Mineralogy of kimberlites

The Chicuatite and Chikolongo kimberlite pipes are rich in pyropes and picroilmenites, the latter being strongly predominant; Cr-spinel and Cr-diopside are scarce. The Ochinjau pipe has similar contents and ratios of indicator minerals. The main indicator minerals of the Palue pipe are pyropes and, more seldom, Cr-spinel; picroilmenite was not found. In the Galange I–IV pipes, the contents of indicator minerals differ drastically: The maximum contents were established in Galange II, and the minimum ones, in Galange IV. The Galange I pipe contains chromite–Cr-diopside–pyrope assemblage with scarce picroilmenite. The other pipes bear pyrope-picroilmenite assemblage with Cr-diopside and minor Cr-spinel. Mineral analyses were carried out on a Jeol JXA-50A electron microprobe at Moscow State University following the technique described by Garanin et al. (1984).

Pyrope

Chicuatite pipe. We studied 295 pyrope grains. Most of them are pyropes of lherzolite paragenesis, and the others

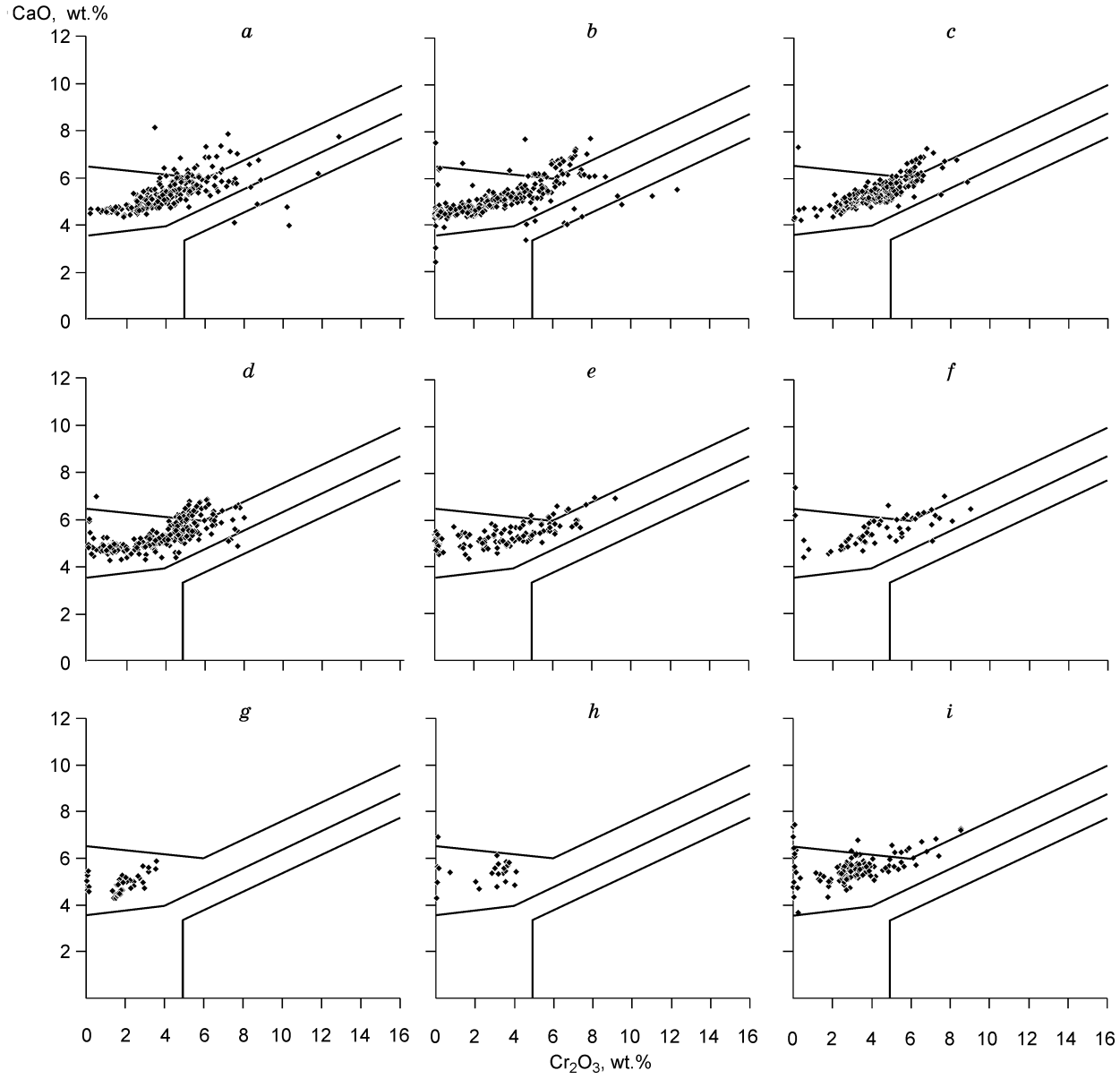

Fig. 5. Cr_2O_3–CaO diagrams for garnets from the kimberlite pipes: *a* — Chicuatite, *b* — Chikolongo, *c* — Palue, *d* — Viniaty, *e* — Ochinjau, *f* — Galange I, *g* — Galange II, *h* — Galange III, *i* — Galange IV.

belong to wehrlite (5%), eclogite (~3%), dunite-harzburgite (2%), and diamond (1%) parageneses. On the Cr_2O_3–CaO diagram (Fig. 5, *a*), the composition points of the Chicuatite pyropes form two trends: The points of one trend are shifted to the field of wehrlite paragenesis pyropes, and the points of the other, to the field of dunite-harzburgite paragenesis pyropes. The maximum content of Cr_2O_3 is 12.8 wt.% (Table 3), the average being 3.5 wt.% ($n = 295$).

Chikolongo pipe. The sample of 302 grains is dominated by pyropes of lherzolite paragenesis (64%); the other grains are garnets of wehrlite (11%) and dunite-harzburgite (including diamond) (~4%) parageneses (Fig. 5, *b*). The maximum content of Cr_2O_3 is 12.34 wt.% (Table 3), the average being 2.5 wt.% ($n = 302$). Garnets with Cr_2O_3 = 0–2 wt.% are the most widespread.

Palue pipe. On the Cr_2O_3–CaO diagram, most of the analyzed grains (n = 221) fall into the composition field of pyropes of lherzolite paragenesis; 16% of the grains belong to wehrlite paragenesis; and 2 grains, to dunite-harburgite paragenesis (Fig. 5, *c*). The average Cr_2O_3 content of the Palue pyropes is 4.2 wt.%.

Viniaty pipe. The analyzed sample (n = 408) includes pyropes of different parageneses with wide variations in Cr_2O_3, CaO, and TiO_2 contents (Fig. 5, *d*). Pyropes of lherzolite paragenesis are predominant (85%). About 10% of the pyropes belong to wehrlite paragenesis, and <1%, to dunite-harzburgite one. The latter are rich in Cr_2O_3 (>7 wt.%) (Table 3), thus being similar to the pyropes of diamond paragenesis. About 4% of the pyropes belong to eclogite paragenesis.

Ochinjau pipe. Among the analyzed pyrope grains (n = 143), 15% belong to titanium mineral assemblage of ultrabasic

Table 3
Microprobe analyses of Cr-pyropes from kimberlite pipes of southwestern Angola (wt.%)

Oxide	Chikolongo pipe							Chicuatite pipe				
SiO_2	39.85	40.17	40.62	40.65	41.37	40.7	41.9	40.35	39.54	40.78	41.43	40.95
TiO_2	0.39	0.28	0.38	0.23	0.08	0.51	0.15	0.11	0.91	0.26	0.22	0.02
Al_2O_3	14.30	15.08	16.47	16.60	16	16.94	17.97	14.72	13.32	16.77	16.78	15.87
Cr_2O_3	12.34	11.09	9.29	9.52	9.56	8.68	7.48	11.75	12.80	8.82	8.66	10.19
FeO	5.84	6.55	6.42	6.07	6.48	6.85	6.46	6.12	7.01	6.31	6.12	6.05
MnO	0.31	0.28	0.24	0.33	0.27	0.27	0.26	0.22	0.33	0.30	0.28	0.26
MgO	20.51	20.34	20.43	21.00	20.77	19.7	21.09	20.10	17.78	19.91	21.70	21.06
CaO	5.52	5.25	5.24	4.86	4.93	6.05	4.37	6.14	7.74	5.87	4.83	4.71
Total	99.06	99.04	99.09	99.26	99.46	99.7	99.68	99.51	99.43	99.02	100.02	99.07
	Chicuatite pipe		Viniaty pipe		Ochinjau pipe		Galange I pipe		Palue pipe		Galange IV pipe	
SiO_2	41.60	41.13	40.82	41.28	40.53	40.40	40.22	41.69	41.47	40.75	41.41	40.8
TiO_2	0.19	0.06	0.11	0.08	0.28	0.82	0.11	0.16	0.22	0.12	0	0.56
Al_2O_3	16.18	18.48	18.25	18.16	17.16	18.07	18.68	18.07	17.03	17.47	16.03	17.46
Cr_2O_3	10.29	7.50	7.59	7.14	9.19	7.42	8.09	7.43	8.81	7.58	8.55	7.42
FeO	5.68	6.82	6.2	6.22	6.67	6.49	7.31	6.01	5.59	6.98	6.46	6.39
MnO	0.28	0.37	0.32	0.25	0.08	0.08	0.24	0.28	0.22	0.32	0.47	0.25
MgO	21.19	21.12	20.91	20.79	19.48	20.77	19.83	19.52	20.02	19.42	19.63	20.09
CaO	3.92	4.04	4.87	5.08	6.93	5.69	5.96	6.09	5.73	6.36	7.28	6.11
Total	99.33	99.52	99.07	99.1	100.32	99.74	100.44	99.25	99.09	99.0	99.83	99.08

Note. Here and in Tables 4–6, total iron is as FeO; Na_2O content was not determined.

paragenesis and are associated with pyrope-ilmenite ultrabasites. They are red-orange and have low contents of Cr_2O_3 (<3.5 wt.%) and high contents of FeO (7–9 wt.%) (Table 3) and TiO_2 (0.48–0.8 wt.%). More than a half of the studied pyropes belong to chromium mineral assemblage of ultrabasic paragenesis. These are violet and crimson pyropes with FeO < 8 wt.% (Table 3).

On the Cr_2O_3–CaO diagram, the pyropes of titanium and chromium mineral assemblages fall into the composition field of lherzolite paragenesis, with 12% of them being rich in Cr_2O_3 (Fig. 5, *e*). Pyropes of dunite-harzburgite paragenesis are lacking, and garnets of wehrlite paragenesis amount to no more than 4%.

The orange pyropes and pyrope-almandines belong to eclogite paragenesis and amount to ~30% of the analyzed garnet grains. These are Ca-pyropes with FeO = 12–15 wt.%, $TiO_2 \approx 1$ wt.%, and $Cr_2O_3 < 0.1$ wt.%.

Galange I pipe. The analyzed pyropes (n = 59) have low to medium contents of Cr_2O_3 and medium contents of CaO (Table 3). Only occasional grains have Cr_2O_3 = 7–9 wt.%. On the Cr_2O_3–CaO diagram, the garnets fall into the composition fields of lherzolite and, to a smaller extent, wehrlite parageneses. One grain belongs to dunite-harzburgite paragenesis (Fig. 5, *f*). It is rich in TiO_2 (>1 wt.%) and FeO (>10 wt.%) and is associated with pyrope-ilmenite ultrabasites. Most grains (76%) are medium-Cr_2O_3 (<5 wt.) pyropes.

Galange II pipe. On the Cr_2O_3–CaO diagram, all pyropes (n = 52) fall into the composition field of lherzolite paragenesis (Fig. 5, *g*) and have medium contents of Cr_2O_3 (<5 wt.%). Large grains of orange garnets of eclogite paragenesis are scarce. These are Ca-pyrope-almandines with high contents of FeO and low contents of Cr_2O_3; they amount to ~18% of all studied garnet grains. Pyropes of diamond paragenesis were not found.

Galange III pipe. On the Cr_2O_3–CaO diagram, almost all (n = 23) analyzed pyrope grains fall into the field of lherzolite paragenesis (Fig. 5, *h*). Orange pyrope-almandines amount to 26% of all garnet grains. Pyropes of diamond paragenesis are lacking.

Galange IV pipe. By the Cr_2O_3–CaO correlation, 76% (n = 75) of the analyzed garnets are assigned to Cr-pyropes of ultrabasic paragenesis (Fig. 5, *i*). Most grains fall into the composition field of lherzolite paragenesis, part of them is high-Cr_2O_3 (>5 wt.%) garnets (Table 3). The composition points of ~6% of the grains lie in the field of wehrlite paragenesis. Pyropes of dunite-harzburgite (including diamond-bearing) paragenesis were not found. Yellow-orange pyrope-almandines amount to ~4% of the analyzed garnet grains.

Picroilmenite

Chicuatite pipe. Picroilmenites (n = 40) have low contents of MgO and Cr_2O_3 (Fig. 6, *a*, *b*): MgO = 6.4–12.17 wt.% and Cr_2O_3 = 0.02–2.5 wt.%; Fe_2O_3 = 7–15 wt.%. They are subdivided into two groups (Table 4): (1) with high contents of TiO_2 (51–55 wt.%) and MgO (8–12 wt.%) and low content of FeO (32–39 wt.%); (2) with low contents of TiO_2 (47–50 wt.%) and MgO (6–8 wt.%) and high content of FeO

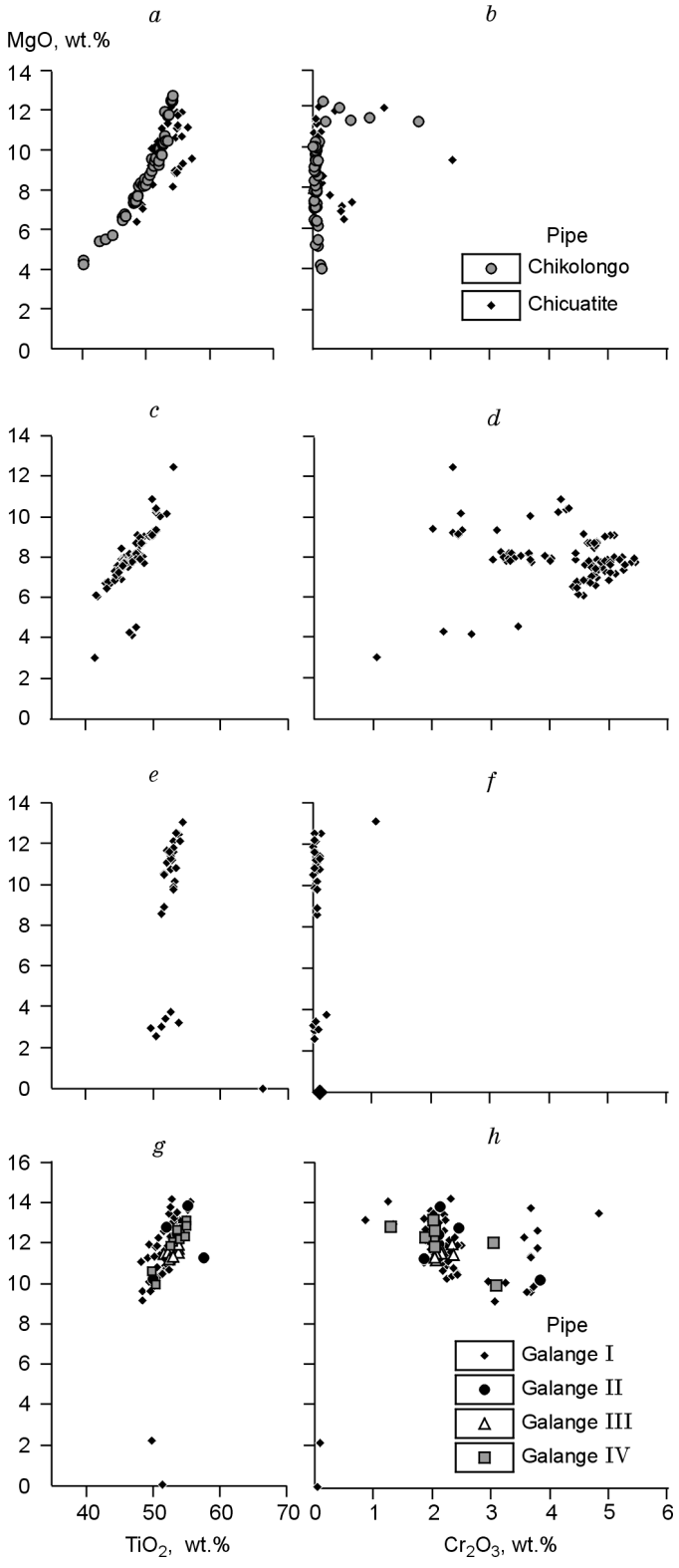

Fig. 6. TiO_2–MgO and Cr_2O_3–MgO diagrams for picroilmenites from the kimberlite pipes: *a*, *b* — Chicuatite and Chikolongo, *c*, *d* — Viniaty, *e*, *f* — Ochinjau, *g*, *h* — Galange I–IV.

(40–44 wt.%). Group 1 picroilmenites are predominant (~80% of the analyzed grains).

Chikolongo pipe. In chemical composition these picroilmenites (n = 52) are very similar to the Chicuatite ones (Fig. 6, *a*, *b*). They are also subdivided into two groups (Table 4): (1) with high contents of TiO_2 (50–54 wt.%) and MgO (8–12.5 wt.%) and low content of FeO (30–40 wt.%); (2) with low contents of TiO_2 (40–49 wt.%) and MgO (4–8 wt.%) and high content of FeO (41–53 wt.%). Group 1 picroilmenites amount to ~60% of the analyzed grains.

In TiO_2–MgO and Cr_2O_3–MgO correlations the Chikolongo and Chicuatite picroilmenites are similar to those of diamondiferous kimberlites from northeastern Angola (Khar'kiv et al., 1998) and differ only in having lower contents of Cr_2O_3 and MgO.

Viniaty pipe. These picroilmenites (n = 92) show a wide variation in contents of MgO (3.02–12.46 wt.%) and TiO_2 (36.98–52.07 wt.%). On the TiO_2–MgO and Cr_2O_3–MgO diagrams, most composition points fall into the field with TiO_2 = 42–48 wt.% and MgO = 6.5–9 wt.% (Fig. 6, *c*, *d*). The picroilmenites are rich in Cr_2O_3 (2–5.2 wt.%) (Table 4).

Ochinjau pipe. Studied picroilmenites (n = 29) are rich in MgO (8–12 wt.%) and poor in Cr_2O_3 (0–0.11 wt.%) (Table 4, Fig. 6, *e*, *f*). Hematite component amounts to 3–5%. Low-Cr_2O_3 picroilmenites of similar composition were earlier found in eclogites and websterites. On the TiO_2–MgO diagram, they fall into the field of highly magnesian picroilmenites from the Mir pipe kimberlites (Yakutia) (Garanin et al., 1984).

Galange I–IV pipes contain picroilmenites (n = 84) of similar chemical composition. They have high contents of MgO (10–15 wt.%) and Cr_2O_3 (1–4.72 wt.%) and no more than 4–9% hematite component (Fig. 6, *g*, *h*). High-Cr_2O_3 picroilmenite of similar composition was earlier found in metasomatized peridotites (Garanin, 1989). Picroilmenites from the Galange I–IV pipes differ considerably from the Chicuatite and Chikolongo ones and those of diamondiferous kimberlites from northeastern Angola (Khar'kiv et al., 1998) in having high contents of MgO and Cr_2O_3 and low content of hematite component (Table 4).

Comparative analysis of the TiO_2, MgO, and Cr_2O_3 contents of picroilmenites from Southwest Angola kimberlite pipes confirmed Sobolev's (1980) conclusion that picroilmenites within the same kimberlite field are similar in average composition, whereas those from different kimberlite fields differ considerably.

Cr-spinel

We failed to study the chemistry of Cr-spinels from the Chicuatite and Chikolongo pipes because of their low contents there.

Palue pipe. A specific chemical feature of Cr-spinels (n = 104) is a narrow range of Cr_2O_3 contents, a predominance of high-Cr_2O_3 high-MgO varieties, and the presence of high-FeO varieties rich in TiO_2 and poor in Al_2O_3, which correspond in composition to ferrichromites (Table 5). Cr-spinels of diamond paragenesis are lacking (Fig. 7, *a*, *b*).

Viniaty pipe. Among the studied Cr-spinels (n = 18), there are many high-Cr_2O_3 varieties; also, ferrichromites occur

Table 4
Microprobe analyses of picroilmenites from kimberlite pipes of southwestern Angola (wt.%)

Oxide	Chicuatite pipe						Chikolongo pipe					
TiO_2	51.11	51.08	55.66	48.53	48.67	53.87	46.41	48.47	49.17	50.99	52.90	54.23
Al_2O_3	0.34	0.58	0.65	0.20	0.36	0.85	0.38	0.43	0.53	0.58	1.17	0.68
Cr_2O_3	0.07	0.05	0.11	0.55	0.30	0.22	0.08	0.04	0.06	0.04	0.98	0.18
FeO	39.95	37.84	31.28	44.08	42.05	32.39	45.87	42.03	40.79	38.02	33.10	31.58
MnO	0.29	0.29	0.23	0.19	0.27	0.21	0.23	0.26	0.30	0.28	0.27	0.63
MgO	8.27	9.63	11.94	6.40	7.62	12.17	6.35	7.31	8.23	9.44	11.82	12.62
Total	100.03	99.49	99.87	99.96	99.34	99.78	99.32	98.54	99.08	99.35	100.24	99.92
	Viniaty pipe		Ochinjau pipe		Galange I pipe		Galange II pipe		Galange III pipe		Galange IV pipe	
TiO_2	44.00	44.87	54.06	52.96	55.31	57.64	53.92	53.88	53.73	52.72	53.30	50.83
Al_2O_3	0.19	0.18	0.70	0.44	0.27	0.39	0.10	0.13	0.27	0.42	0.47	0.00
Cr_2O_3	4.50	4.65	0.03	0.00	2.11	1.85	2.13	2.15	2.03	4.72	1.84	2.36
FeO	43.26	42.63	32.59	33.50	28.71	29.17	31.21	31.18	30.20	29.34	29.75	32.52
MnO	0.26	0.33	0.22	0.31	0.20	0.19	0.32	0.41	0.37	0.39	0.35	0.29
MgO	6.80	7.28	12.17	11.84	13.83	11.27	11.72	11.53	12.66	11.86	13.27	12.31
Total	99.01	99.94	99.77	99.07	100.43	100.51	99.40	99.40	99.30	99.45	99.37	99.22

Table 5
Microprobe analyses of Cr-spinels from kimberlite pipes of southwestern Angola (wt.%)

Oxide	Palue pipe						Viniaty pipe					
TiO_2	0.77	1.73	0.16	3.60	1.66	2.96	2.16	0.63	1.24	2.51	1.95	0.64
Al_2O_3	13.21	12.10	12.72	6.48	17.30	9.74	5.58	7.96	4.09	4.54	9.33	10.55
Cr_2O_3	55.95	54.22	58.87	51.24	44.99	49.06	60.72	59.06	63.17	61.48	55.16	58.02
FeO	17.17	20.28	16.11	27.62	22.22	24.88	21.55	23.13	22.43	20.93	24.46	19.50
MnO	0.22	0.15	0.15	0.30	0.14	0.35	0.37	0.28	0.36	0.29	0.42	0.27
MgO	11.99	10.50	11.27	9.67	12.74	11.64	9.31	8.84	8.20	9.57	7.94	10.29
Total	99.42	99.11	99.30	99.03	99.17	99.42	99.69	99.90	99.49	99.32	99.26	99.27
	Galange I pipe						Galange II pipe					
TiO_2	2.84	4.53	1.78	0.13	0.25	3.84	0.88	0.39	0.17	3.16	2.82	2.90
Al_2O_3	2.27	9.69	1.67	15.22	14.16	11.65	16.50	16.21	15.70	2.87	3.17	2.10
Cr_2O_3	53.67	49.76	50.47	51.25	52.14	48.68	47.19	48.72	50.81	53.30	54.83	55.14
FeO	33.93	23.10	33.75	20.97	20.90	21.70	21.99	20.30	18.91	29.13	28.40	29.45
MnO	0.04	0.19	4.44	0.15	0.11	0.20	0.20	0.27	0.28	0.32	0.33	0.03
MgO	7.02	12.14	8.14	12.58	12.16	13.60	12.30	13.01	13.10	10.52	9.87	9.60
Total	99.77	99.41	100.25	100.30	99.72	99.72	99.13	99.02	99.06	99.52	99.58	99.43
	Galange III pipe						Galange IV pipe					
TiO_2	0.10	0.19	0.59	1.24	3.61	4.45	1.03	0.26	0.90	1.58	0.41	4.81
Al_2O_3	15.75	8.16	16.70	9.74	2.31	8.63	13.70	16.01	9.94	13.16	20.09	3.29
Cr_2O_3	51.21	56.88	49.32	47.48	51.51	50.44	48.60	50.54	55.50	53.39	44.49	49.68
FeO	20.21	22.43	19.23	29.17	32.92	22.07	21.59	20.0	20.64	19.15	23.04	29.94
MnO	0.26	0.39	0.24	0.31	0.40	0.30	0.31	0.20	0.20	0.30	0.20	0.62
MgO	12.55	10.81	12.94	10.91	8.09	13.22	13.55	13.50	12.48	12.02	12.28	10.34
Total	100.13	99.0	99.17	99.03	99.12	99.11	99.08	100.75	99.66	99.50	100.51	99.03

(Fig. 7, *c*, *d*). Varieties of diamond paragenesis are lacking, though almost all analyzed Cr-spinels are rich in Cr_2O_3 (Table 5).

Galange I–IV pipes contain compositionally similar Cr-spinels (n = 129). They show wide variations in contents of Al, Mg, and Ti and narrow ranges of Cr contents. The samples are dominated by highly magnesian chromites and magnesian aluminochromites. There are also high-FeO varieties rich in TiO_2 and poor in Al_2O_3, which compositionally correspond to ferrichromites (Table 5, Fig. 7, *e*, *f*). Cr-spinels of diamond paragenesis are lacking.

Diopside

Diopsides occur as elongate-oval angular grains 0.5–4.00 mm in size. Grains with fragments of myriahedral habit faceting are scarce. Sometimes, diopsides are intergrown with

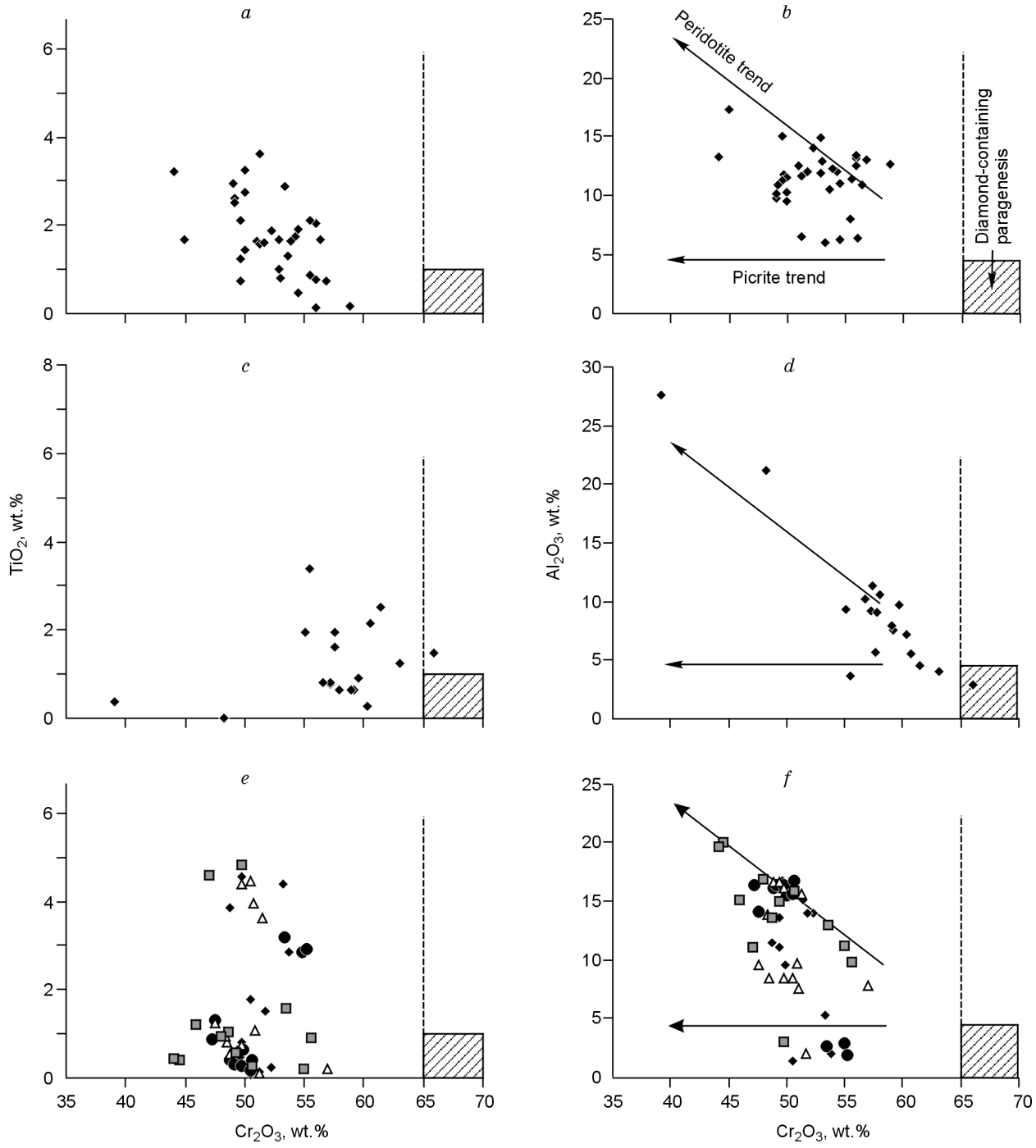

Fig. 7. Cr_2O_3–TiO_2 and Cr_2O_3–Al_2O_3 diagrams for Cr-spinels from the kimberlite pipes: *a*, *b* — Palue, *c*, *d* — Viniaty, *e*, *f* — Galange I–IV. Designations follow Fig. 6, *g*, *h*.

pyrope, phlogopite, and pseudomorphs after olivine. Kimberlites from the southern pipe group are most enriched in pale-green to bright-emerald diopside phenocrysts.

The analyzed diopside grains (n = 27) from the Galange I–III kimberlites are characterized by similar chemical compositions (Fig. 8, *a*, *b*). Pale-green diopsides have low contents of Cr_2O_3 (<1 wt.%) and Na_2O (<1 wt.%) (Table 6). By composition, they can be referred to as Cr-containing subcalcic clinopyroxenes of spinel-pyroxene facies (Sablukov et al., 2000). Emerald-green varieties are enriched in Cr_2O_3 and have variable contents of Na_2O and Al_2O_3. According to the Na_2O/Al_2O_3 ratio, they belong to Cr-diopsides of grospydite and coesite facies. Occasional diopside grains have high contents of Al_2O_3 (>4 wt.%) and low contents of Na_2O, Cr_2O_3, and FeO. According to the correlations between these components, the grains fall into the composition field of diopsides of low-pressure spinel-pyroxene facies. Such clinopyroxenes are typical of spinel lherzolites associated with picotite and Cr-picotite; the latter two often occur in the Galange II kimberlites. Pressure calculations using the Nimis–

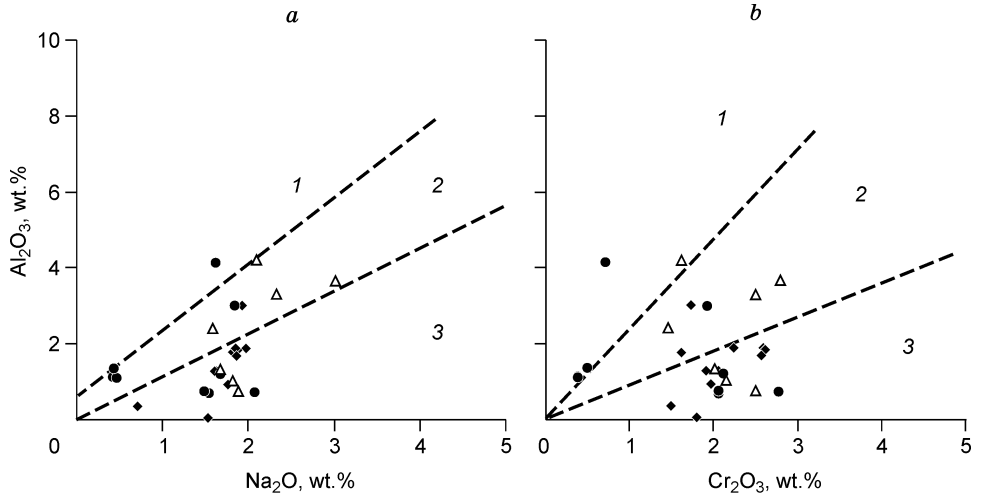

Fig. 8. Na_2O–Al_2O_3 (*a*) and Cr_2O_3–Al_2O_3 (*b*) diagrams for diopsides from the Galange I–III kimberlites. Facies: *1* — spinel-pyroxene, *2* — grospydite, *3* — coesite, after Sablukov et al. (2000). Designations follow Fig. 6, *g*, *h*.

Taylor Cr barometer (Nimis and Taylor, 2000) showed that clinopyroxenes of the Galange I and Galange III pipes formed at 26.8–50.8 kbar, whereas the Galange II clinopyroxenes were produced in a wider pressure range, 13.7–53.8 kbar.

By the Cr_2O_3–FeO and MgO–FeO correlations, the composition points of the analyzed diopside grains generally fit the composition trend of clinopyroxenes from the South African group I kimberlites (Garanin, 1989). Such diopsides are genetically related to lherzolites, pyroxenites, and ilmenite peridotites.

The studied Cr-diopsides differ from those from Northeast Angola diamond pipes in having lower contents of Cr_2O_3 (<3 wt.% against 4.5 wt.%, respectively) and Na_2O (<3 wt.% against 3–6.3 wt.%).

Diamonds

Diamonds 1.5 to 4.5 mm in size and 0.01 to 0.14 carats in weight were found as single crystals, their fragments, and intergrowths of two and more crystals in the Chicuatite and Chikolongo pipes. Most crystals are of rhombododecahedral habit and rhombododecahedroids. The Chicuatite diamonds are rhombododecahedra and their fragments. The Chikolongo diamonds are, on the contrary, crystals of transitional habit of the sequence octahedron–dodecahedron and crystals of uncertain shape. Cubes and tetrahexahedroids were not found. According to the classification of Orlov (1984), all crystals belong to group I. Many of them are of disturbed symmetry. Most crystals are strongly flattened along the L_3 and L_2 symmetry axes. The diamonds are mainly colorless or slightly yellowish, and five crystals are brown. All diamond crystals bear traces of partial dissolution, expressed as micronodes forming a shagreen topography and as etching pits of triangular and square sections.

Thus, the Chicuatite and Chikolongo kimberlite pipes (northern group of pipes) are characterized by a wide spectrum of indicator-mineral compositions (different types of parageneses), the presence of pyropes of dunite-harzburgite (including diamond-bearing) paragenesis and picroilmenites compositionally similar to those from diamond-bearing kimberlites of northeastern Angola. The content of high-Cr low-Ca pyropes

Table 6
Microprobe analyses of clinopyroxenes from kimberlite pipes of southwestern Angola (wt.%)

Oxide	Galange I pipe						Galange II pipe			Galange III pipe		
SiO_2	55.09	54.85	53.90	54.22	54.19	54.72	54.35	54.95	54.53	53.37	54.24	54.29
TiO_2	0.28	0.40	0.35	0.37	0.11	0.23	0.09	0.34	0.27	0.51	0.21	0.21
Al_2O_3	0.93	1.28	1.89	1.84	3.01	1.69	3.00	1.21	0.72	4.20	3.30	3.67
Cr_2O_3	1.97	1.92	2.60	2.62	1.73	2.57	1.93	2.12	2.78	1.62	2.51	2.80
FeO	2.60	2.64	2.38	2.37	2.50	2.40	2.41	2.64	3.13	1.48	2.39	2.30
MnO	0.09	0.11	0.11	0.07	0.12	0.00	0.02	0.03	0.00	0.01	0.00	0.00
MgO	15.38	15.81	15.40	15.40	15.51	16.05	15.72	16.20	15.45	15.06	15.51	15.02
CaO	21.06	20.86	19.90	19.83	20.29	20.38	20.21	20.39	20.30	21.01	19.40	18.44
Na_2O	1.76	1.63	1.97	1.87	1.93	1.86	1.84	1.67	2.07	2.10	2.33	3.01
K_2O	0.10	0.00	0.00	0.01	0.00	0.04	0.04	0.05	0.00	0.05	0.08	0.05
Total	99.26	99.50	98.50	98.60	99.39	99.94	99.61	99.60	99.25	99.42	99.98	99.79

is in positive correlation with the rock diamond potential, which confirms the general regularities established earlier by Sobolev for kimberlites of northeastern Angola (Sobolev et al., 1990) and Yakutia (Sobolev, 1977). The revealed relationship between the presence of pyropes of diamond-bearing dunite-harzburgite paragenesis and diamonds in kimberlites from southwestern Angola confirms that this mineralogical criterion used to estimate the diamond potential of kimberlites and lamproites is quite universal (Sobolev, 1971).

The central-group kimberlite pipes (Palue, Viniaty, Ochinjau) are characterized by a strong predominance of minerals of chromium assemblages over minerals of titanium assemblage of ultrabasic paragenesis. But the absence of pyropes of diamond assemblage from the studied sample casts doubt on the presence of diamonds in these kimberlites. Note that the kimberlite Cr-spinels show a narrow range of Cr_2O_3 contents and are dominated by high-Cr varieties.

The southern-group kimberlite pipes (Galange I–IV) are characterized by a strong predominance of medium-Cr_2O_3 pyropes of lherzolite paragenesis, a narrow range of Cr_2O_3 contents of Cr-spinels (45–55 wt.%), the absence of grains of diamond assemblage among pyropes and Cr-spinels, and high Cr_2O_3 contents and Mg# values of picroilmenites. The Cr_2O_3-richest pyropes (up to 9 wt.% Cr_2O_3) were found in the Galange I and Galange IV pipes.

Conclusions

Results of our complex studies of unknown kimberlite pipes permitted us to recognize a new diamondiferous kimberlite province within southwestern Angola.

By all lithologic and indication parameters, the studied kimberlites are referred to as classical kimberlites: They contain mantle inclusions of ultrabasites and eclogites, an entire spectrum of barophilic minerals, including ones of diamond facies, and diamonds. The kimberlite pipes are composed of rocks of different types: tuffstones, tuff breccias, kimberlite breccias, autolithic kimberlite breccias, and massive porphyritic kimberlites. The kimberlites are differently contaminated by the material of intruded rocks and are strongly transformed by hydrothermal-metasomatic and hypergene processes. Nevertheless, the contents of major and trace components in the pipe rocks are commensurate with those in kimberlites of other world's regions. In mineralogical, petrographic, and petrochemical compositions the studied kimberlites are similar to South African group I kimberlites and Fe-Ti-kimberlites of the Arkhangel'sk diamondiferous province. We have first revealed kimberlites of Paleozoic age in southwestern Angola.

Comparison of the mineralogical compositions of kimberlites from southwestern Angola shows a regular increase in the portion of mantle (including diamond-bearing) material of depth facies in the kimberlite pipes in the S-N direction. A similar regularity is observed for kimberlite bodies in northeastern Angola (Zuev et al., 1988), localized in zone of W-E-striking deep faults up to 1600 km in total length. This might account for why diamond-bearing kimberlites of the northern pipe group are localized in large destructive zones of NE strike and diamond-free kimberlite pipes of the central and southern pipe groups, in N-S-striking faults (Fig. 1).

We thank Academician N.V. Sobolev for valuable constructive remarks on the manuscript.

References

Bogatikov, O.A., Garanin, V.K., Kononova, V.A., et al., 2000. Arkhangel'sk diamondiferous province [in Russian]. Nauka, Moscow.

Bogatikov, O.A., Kononova, V.A., Golubeva, Yu.Yu., Zinchuk, N.N., Ilupin, I.P., Rotman, A.Ya., Levsky, L.K., Ovchinnikova, G.V., Kondrashov, I.A., 2004. Petrochemical and isotopic variations of compositions of Yakutian kimberlites and their reasons. Geokhimiya 9, 915–939.

Bogatikov, O.A., Kononova, V.A., Pervov, V.A., Zhuravlev, D.Z., 2001. Sources, geodynamic setting of formation, and diamond potential of kimberlites on the Russian Plate margin: Sr-Nd isotopy and ICP MS geochemistry. Petrologiya 9 (3), 227–241.

Garanin, V.K., 1989. Introduction to geology of diamond deposits [in Russian]. Izd. Moskovskogo Universiteta, Moscow.

Garanin, V.K., Kudryavtseva, G.P., Soshkina, L.T., 1984. Ilmenite from kimberlites [in Russian]. Izd. Moskovskogo Universiteta, Moscow.

Khar'kiv, A.D., Zinchuk, N.N., Kryuchkov, A.I., 1998. World's primary diamond deposits [in Russian]. Nedra, Moscow.

McDonough, W.F., Sun, S.S., 1995. The composition of the Earth. Chem. Geol. 120, 223–253.

Nimis, P., Taylor, W.R., 2000. Single clinopyroxene thermobarometry for garnet peridotites: Part 1. Calibration and testing of a Cr-in-Cpx barometer and an enstatite-in-Cpx barometer. Contr. Miner. Petrol. 139 (5), 541–554.

Orlov, Yu.L., 1984. Diamond mineralogy [in Russian]. Nauka, Moscow.

Roman'ko, E.F., Egorov, K.N., Podvysotskii, V.T., Sablukov, S.M., D'yakonov, D.B., 2005. A new diamondiferous kimberlite region in southwestern Angola. Dokl. Earth Sci. 403A (6), 817–821.

Sablukov, S.M., Sablukova, L.I., Shavyrina, M.V., 2000. Mantle xenoliths from kimberlite rounded-diamond deposits of the Zimnii Bereg region, Arkhangel'sk diamondiferous province. Petrologiya 8 (5), 518–548.

Sobolev, N.V., 1971. Mineralogical criteria for kimberlite diamond potential. Geologiya i Geofizika (3), 70–80.

Sobolev, N.V., 1977. Deep seated inclusions in kimberlites and the problem of the composition of the upper mantle. AGU, Washington, DC.

Sobolev, N.V., 1980. Significance of picroilmenite for locating kimberlite fields. Geologiya i Geofizika (Soviet Geology and Geophysics) (10), 149–151 (127–129).

Sobolev, N.V., Mankenda, A., Kaminsky, F.V., Sobolev, V.N., 1990. Garnets from kimberlites of northeastern Angola and their composition–diamond potential relationship. Dokl. Akad. Nauk SSSR 315, 1225–1229.

Taylor, W.R., Tompkins, L.A., Haggerty, S.E., 1994. Comparative geochemistry of West African kimberlites: evidence for a micaceous kimberlite end member of sublithospheric origin. Geochim. Cosmochim. Acta 58 (19), 4017–4037.

Zuev, V.M., Khar'kiv, A.D., Zinchuk, N.N., Mankenda, A., 1988. Weakly eroded kimberlite pipes of Angola. Geologiya i Geofizika (Soviet Geology and Geophysics) 29 (3), 56–62 (50–57).